



Dynamic Surface-Based Adaptive Fuzzy Fixed-Time Fault-Tolerant Control for Nonstrict Feedback Nonlinear Systems With Non-affine Faults

Yueyang Wang^{1,2,3} · Zhumu Fu^{1,2} · Fazhan Tao³ · Nan Wang^{1,2,3} · Zhengyu Guo⁴

Received: 6 August 2022 / Revised: 29 January 2024 / Accepted: 28 February 2024 / Published online: 20 April 2024
© The Author(s) under exclusive licence to Taiwan Fuzzy Systems Association 2024

Abstract In the paper, a dynamic surface-based adaptive fuzzy fixed-time fault-tolerant control scheme is developed for nonstrict feedback nonlinear systems with non-affine faults. Firstly, the computational complexity is reduced by adopting dynamic surface control technique, and unknown nonlinear functions are approximated with the help of fuzzy logic systems. Secondly, non-affine faults involving system states and controller output are taken into account and treated by transforming it into nonlinear in the unknown parameters. Then, under the framework of fixed-time stability, a novel adaptive fuzzy fault-tolerant control strategy is designed so that the closed-loop system is semi-globally practically fixed-time stable. Finally, a numerical simulation and a model simulation are given to demonstrate the effectiveness of the proposed control scheme.

Keywords Nonlinear system · Fault-tolerant control · Fixed-time stability · Fuzzy logic systems · Non-affine faults

1 Introduction

In the past few decades, backstepping-based adaptive control has become one of the most popular design methods to deal with nonlinear systems and has obtained many very meaningful results [1, 2]. To give a few examples, with the help of the backstepping-based adaptive neural network technique, [3] solves the asymptotic tracking control problem of high-order fully actuated systems. Based on the research in Zhao et al. [3], a fuzzy state observer is introduced for nonstrict nonlinear systems in [4] to address the unmeasurable state problem and the algebraic loop problem. Since the backstepping method requires repeated differentiation of the virtual controller, the above literatures [3, 4] inevitably have the phenomenon of “complexity explosion” as the order of the system increases. To solve this problem, dynamic surface control technology is used in Wang et al. [5] to successfully reduce the complexity of n -order nonstrict feedback system in the controller design process. In Singh et al. [6], flight path angle of the aircraft is controlled asymptotically for a class of nonstrict feedback system by employing robust backstepping dynamic surface control. Further [7] combines the adaptive dynamic surface method with the gain suppressing inequality technique to solve the predefined tracking control problem of stochastic systems. Although the adaptive dynamic surface control method has a certain degree of robustness to resist external uncertainties, unfortunately, it cannot solve the system dynamics caused by the actuator failure.

In practical engineering, due to the complexity of the working environment and the limitation of the material itself, the actuator will inevitably fail. The existence of faults can seriously damage the system performance and cause adverse effects on economy. Therefore, designing a

✉ Zhumu Fu
fuzhumu@haust.edu.cn

✉ Fazhan Tao
taofazhan@haust.edu.cn

¹ College of Information Engineering, Henan University of Science and Technology, Luoyang 471023, Henan, China

² Key Laboratory of Robot and Intelligent System of Henan Province, Henan University of Science and Technology, Luoyang 471023, Henan, China

³ Longmen Laboratory, Luoyang 471023, Henan, China

⁴ Aviation Key Laboratory of Science and Technology on Airborne Guided Weapon, China Airborne Missile Academy, Luoyang 471009, Henan, China

reasonable fault-tolerant control scheme to reduce the impact of faults on the system meets the needs of social development. In terms of practical applications, for the supersonic tailless aircraft subject to actuator faults, [8] develops a fault-tolerant scheme based on reconfiguration control allocation. Nevertheless, for the spacecraft attitude control system with actuator faults, [9] presents a fault-tolerant scheme based on iterative learning observer. In addition, compared with the active fault-tolerant control used in Cong et al. [8, 9], the passive fault-tolerant control scheme is adopted in Shi et al. [10] for the three-phase machine system, which speeds up system response. In terms of theoretical research, for polynomial fuzzy systems with linear actuator faults, [11] develops a polynomial adaptive fuzzy observer to estimate actuator faults. However, for high-order nonlinear system with non-affine nonlinear faults, [12] constructs a new adaptive fuzzy fault-tolerant controller based on the high-order fully actuated systems theory. Considering that multi-agent systems are vulnerable to malicious attacks during communication, [13] proposes an adaptive collaborative fault-tolerant control scheme based on distributed sliding mode observer. The above literatures only focus on the steady-state performance of the system. In fact, the convergence rate is also an important factor affecting the industrial production. Therefore, it is necessary to develop a control scheme that considers both stability and convergence rate.

The fixed-time control can take into account both the steady-state performance and the convergence rate of the system. Compared with the finite-time control, it gets rid of the dependence on the initial conditions. In recent years, fixed-time control has received great attention and has been applied in many fields, such as aerospace field [14, 15], robotics field [16, 17], automotive field [14, 18, 19] studies the fixed-time attitude tracking control problem of spacecraft with prescribed performance, and designs a prescribed performance tracking controller based on disturbance observer. [15] further considers the impact of actuator failures on spacecraft based on the findings of [14]. Zhou et al. [16] designed a neural network fixed-time slide mode trajectory controller to adjust the desired angular positions of rigid-flexible coupled robotic mechanisms for the rigid-flexible coupled robotic mechanisms with large beam deflections. To guarantee the transient and steady-state performance of uncertain robotic manipulators within fixed time, an approximate continuous fixed-time terminal sliding mode control with prescribed performance is developed in Sai et al. [17]. Jia et al. [18, 19] studied the adaptive fixed-time control problem of active suspension systems with actuator faults and active suspension systems with time-varying displacement constraints, respectively.

Based on the above paper's inspiration, this paper mainly studies the adaptive fuzzy fixed-time fault-tolerant

control problem for nonstrict feedback nonlinear systems with non-affine faults. Based on the dynamic surface technique, an adaptive fuzzy fixed-time fault-tolerant controller is constructed. The controller can ensure that the tracking error converges to the small neighborhood near the origin regardless of whether the fault exists. The main contributions are as follows:

- (1) For nonlinear systems with actuator failures, an adaptive fuzzy passive fault-tolerant control scheme based on fixed time is proposed. Compared with the active fault-tolerant control scheme in Sha et al. [20], the passive fault-tolerant control strategy proposed is simpler and the response speed is faster. More to the point, the combination of passive fault-tolerant control and fixed-time stability theory ensures the stability and tracking accuracy of the system while retaining the original advantages of passive fault-tolerance.
- (2) Non-affine nonlinear faults causing actuator failure are considered. Different from linear faults in Yang et al. [21, 22], non-affine nonlinear faults are more common in industry. By giving the upper bound of the undivided term composed by the unknown function and the unknown fault function, using the approximation characteristics of fuzzy logic systems (FLSs), the fault-tolerant control problem considered in this paper is reduced to dealing with the unknown bounding function problem.
- (3) In this paper, a more representative nonlinear system with nonstrict feedback structure is considered and the approximation performance of fuzzy logic is used to deal with the nonlinear functions containing all state variables in the system. In addition, the introduction of dynamic surface control technology not only solves the problem of "complexity explosion" in Ha et al. [23], but also avoid the calculation of partial derivatives.

The rest of this paper is organized as follows. Section 2 gives the preliminaries, which are used in the design of the fixed-time fault-tolerant tracking controller. The control strategy and stability analysis are completed in Sect. 3. Section 4 uses two simulations as examples to verify the effectiveness of the proposed scheme. In the end, the conclusion is given in detail in Sect. 5.

2 Problem Statement and Preliminaries

In order to meet the design requirements of the fault-tolerant tracking controller, a nonlinear system model is given, which has nonstrict feedback form and non-affine fault term.

$$\begin{cases} \dot{x}_1 = x_2 + f_1(x) \\ \vdots \\ \dot{x}_i = x_{i+1} + f_i(x) \\ \vdots \\ \dot{x}_n = u + f_n(x) + \zeta(t - T_0)\tau(x, u) \\ y = x_1 \end{cases}, \tag{1}$$

where $x = [x_1, x_2, \dots, x_n] \in \mathfrak{R}^n$, $u \in \mathfrak{R}$, and $y \in \mathfrak{R}$ stand for the state vector, input, and output of system (1), respectively. Given a desired tracking signal y_r , system output y can track desired output y_r well under the action of the developed fault-tolerant tracking controller, and the tracking error is denoted as e and $e = y - y_r$. $f_i(x)$ denotes the smooth nonlinear function, which is unknown in this paper. Some unknown changes may occur due to existing faults in the system, represented by $\tau(x, u)$, where $\tau(x, u) \in \mathfrak{R}$. $\zeta(t - T_0)$ refers to the homologous time profile of the fault that occurs at some unknown time T_0 and can be described by the following two cases:

Case 1: If $t < T_0$ is satisfied, $\zeta(t - T_0)$ can be written as $\zeta(t - T_0) = 0$. (2)

Case 2: If $t \geq T_0$ is satisfied, $\zeta(t - T_0)$ can be written as $\zeta(t - T_0) = 1 - e^{-\varrho(t-T_0)}$, (3)

where ϱ is a non-negative constant that represents the corresponding evolution rate caused by unknown faults.

This paper employs the passive fault-tolerant control scheme based on fixed-time to offset the effects and changes of system non-dynamics caused by faults. Non-affine nonlinear faults involving system state and controller output are considered. When the value of ϱ is relatively small, the fault type of the system is an incipient fault. On the contrary, when the value of ϱ is pretty large, the fault type of the system is an abrupt fault. The passive fault-tolerant control scheme does not require the fault identification and isolation unit, but only evaluates the fault level by designing the corresponding adaptive law. The adaptive law feeds the evaluation results back to the fault-tolerant controller. Then, under the action of fault-tolerant controller, the effects and changes of system non-dynamics caused by faults are weakened.

The following two assumptions are given, which are essential to solving such problems in order to successfully design the controller for a plant with non-affine faults.

Assumption 1 In system (1), the reference signal $y_r(t)$ and its corresponding first-order time derivative $\dot{y}_r(t)$ and second-order time derivative $\ddot{y}_r(t)$ are all bounded and known.

Assumption 2 Given an unknown non-negative function $\bar{h}(x, u)$, such that it satisfies the following equation:

$$|f_n(x) + \zeta(t - T_0)\tau(x, u)| \leq \bar{h}(x, u) \tag{4}$$

Remark 1 Assumption 1 only restricts $y_r(t)$, $\dot{y}_r(t)$, and $\ddot{y}_r(t)$, but does not astrict the remaining n -order time derivatives, where n is an integer greater than 2. The strict constraints on the previous reference signals $y_r(t)$ are relaxed and the computational complexity is reduced. Assumption 2 treats the term $f_n(x)$ and the term $\zeta(t - T_0)\tau(x, u)$ as a whole, called $h(x, u)$. Meanwhile, $h(x, u)$ satisfies the condition $|h(x, u)| \leq \bar{h}(x, u)$. The ultimate purpose of Assumption 1 and Assumption 2 is to simplify the calculation process and reduce the computational complexity. For similar assumptions, see [24–26] for detail.

In order to successfully complete the design task of the fault-tolerant tracking controller, some related Lemmas are introduced.

Lemma 1 (Young’s inequality [27]) For $\forall(x, y) \in \mathfrak{R}^2$, the following inequality holds:

$$xy \leq \frac{\vartheta^m}{m} |x|^m + \frac{1}{n\vartheta^n} |y|^n, \tag{5}$$

where $\vartheta > 0$, $m > 1$, $n > 1$. At the same time, in order for (5) to hold, m and n must also satisfy $(m - 1)(n - 1) = 1$.

Lemma 2 [28] Consider $f_l > 0$, the following inequalities hold:

$$\left(\sum_{l=1}^n f_l\right)^p \leq \sum_{l=1}^n f_l^p \leq n^{1-p} \left(\sum_{l=1}^n f_l\right)^p, \tag{6}$$

$$n^{1-q} \left(\sum_{l=1}^n f_l\right)^q \leq \sum_{l=1}^n f_l^q \leq \left(\sum_{l=1}^n f_l\right)^q, \tag{7}$$

where $0 < p \leq 1$, $q \geq 1$.

Lemma 3 [29] Suppose $V(x)$ satisfies the following conditions: (1) $V(x)$ is a positive definite function; (2) $\dot{V}(x)$ is a negative definite function. If any solution $x(t)$ of the plant (1) satisfies $\dot{V}(x) \leq -sV^\kappa(x) - tV^\iota(x)$, then the system (1) is globally stable in fixed-time, and the setting-time T of the plant (1) is $T \leq T_{\max} = 1/(s(1 - \kappa)) + 1/(t(\iota - 1))$. If $x(t)$ satisfies $\dot{V}(x) \leq -sV^\kappa(x) - tV^\iota(x) + W$, then the system (1) is practically stable in fixed-time, and the setting-time T is $T \leq T_{\max} = 1/(s\eta(1 - \kappa)) + 1/(t\eta(\iota - 1))$. In the above inequality, s , t , κ , ι , η , and W all denote constants, and satisfy $s > 0$, $t > 0$, $0 < \kappa < 1$, $\iota > 1$, $0 < \eta < 1$, and $W > 0$, respectively.

Proof See [30–32] for the proof of Lemma 3.

In this paper, the approximation performance of FLSs is needed to deal with unknown nonlinear functions f in the plant (1), and then be applied to dynamic surface control technique to design the desired controller. FLSs can be divided into four parts: knowledge base, fuzzifier, fuzzy inference engine, and defuzzifier. The knowledge base of FLSs is composed of a set of If-Then rules, as follows:

χ^k : If χ_1^k is Ψ_1 and χ_2^k is Ψ_2 and... and χ_n^k is Ψ_n , then y is Φ^k , $k = 1, 2, \dots, n$. Here, $\chi = [\chi_1, \chi_2, \dots, \chi_n]^T$ represents the input vector of FLSs, y refers to the output of FLSs. $\mu\Psi_i^k(\chi_i)$ and $\mu\Phi^i(\chi_i)$ are defined on fuzzy sets Ψ_i^k and Φ^i , respectively. $\mu\Psi_i^k(\chi_i)$ and $\mu\Phi^i(\chi_i)$ are called membership functions. N denotes the number of rules. Therefore, the output expression of FLSs can be written in the following form:

$$y(\chi) = \frac{\sum_{k=1}^N \vartheta_k \prod_{i=1}^n \mu\Psi_i^k(\chi_i)}{\sum_{k=1}^N \left(\prod_{i=1}^n \mu\Phi^i(\chi_i) \right)}, \tag{8}$$

where $\vartheta_k = \max y \in \mu\Phi^k(y)$, $\varpi = [\vartheta_1, \vartheta_2, \dots, \vartheta_N]^T = [\varpi_1, \varpi_2, \dots, \varpi_N]^T$. The basis functions are defined as

$$\varphi_k(\chi) = \frac{\prod_{i=1}^n \mu\Psi_i^k(\chi_i)}{\sum_{k=1}^N \left(\prod_{i=1}^n \mu\Phi^i(\chi_i) \right)}. \tag{9}$$

Let $\varphi(\chi) = [\varphi_1(\chi), \varphi_2(\chi), \dots, \varphi_N(\chi)]$, one can get

$$y(\chi) = \varpi^T \varphi(\chi). \tag{10}$$

Lemma 4 [33] *Suppose there exists an unknown nonlinear function f that is smooth and defined on the complete set Π . FLSs can be expressed in the following form:*

$$\sup_{\chi \in \Pi} |f(\chi) - \varpi^{*T} \varphi(\chi)| \leq \epsilon, \tag{11}$$

where ϖ^{*T} stands for the ideal weight vector, ϵ is the approximation error, which is a constant and satisfies $\epsilon > 0$. It is worth noting that the smaller ϵ is, the higher the approximation accuracy of FLSs is.

The unknown nonlinear function $f_i(\chi)$, $i = 1, 2, \dots, n$ is expressed as the following form according to the content of Lemma 4.

$$f_i(\chi | \varpi) = \varpi_i^T \varphi(\chi). \tag{12}$$

Then the ideal weight vector ϖ^* and approximation error ϵ can be expressed as

$$\varpi_i^* = \arg \min_{\varpi_i \in \Pi_i} \left\{ \sup_{\chi_i \in \Pi_i} |f_i(\chi | \varpi_i) - f_i(\chi)| \right\}. \tag{13}$$

$$\epsilon_i = f_i(\chi) - f_i(\chi | \varpi_i^*), \tag{14}$$

ϖ^* , $\hat{\varpi}$, and $\tilde{\varpi}$ are defined as the corresponding ideal weight vector, estimation vector, and estimation error, respectively. Meanwhile, the relationship among the three is $\tilde{\varpi} = \varpi^* - \hat{\varpi}$.

3 Control Strategy and Stability Analysis

In this section, the design work of the controller is executed. The paper uses dynamic surface technique to construct the controller, with its coordinate transformation as follows: $e_1 = y - y_r$, $e_i = x_i - \omega_i$, $\eta_i = \omega_i - \alpha_{i-1}$, $i = 2, \dots, n$. Different from the backstepping method, the dynamic surface method employed in this paper uses ω_i instead of $\dot{\alpha}_{i-1}$ in each step so that simple algebraic operations replaced the original complex differential operations, simplifying the derivation process of the controller.

3.1 Control Strategy

Step 1: According to the above coordinate transformations and the plant (1), we can get the following formula:

$$\dot{e}_1 = e_2 + \eta_2 + \alpha_1 + f_1(x) - \dot{y}_r. \tag{15}$$

Since $f_1(x)$ is an unknown nonlinear function, it can be approximated by FLSs. According to formulas (12), (14), and $\tilde{\varpi}_1 = \varpi_1^* - \hat{\varpi}_1$, we can get $f_1(x) = \epsilon_1 + \tilde{\varpi}_1^T \varphi_1(x) + \hat{\varpi}_1^T \varphi_1(x)$. Therefore, (15) can be rewritten as

$$\dot{e}_1 = e_2 + \eta_2 + \alpha_1 + \epsilon_1 + \tilde{\varpi}_1^T \varphi_1(x) + \hat{\varpi}_1^T \varphi_1(x) - \dot{y}_r. \tag{16}$$

Considering the Lyapunov function $V_1 = \frac{1}{2} e_1^2 + \frac{1}{2r_1} \tilde{\varpi}_1^T \tilde{\varpi}_1$, its time derivative can be obtained

$$\begin{aligned} \dot{V}_1 = & e_1(e_2 + \eta_2 + \alpha_1 + \epsilon_1 + \tilde{\varpi}_1^T \varphi_1(x) \\ & + \hat{\varpi}_1^T \varphi_1(x) - \dot{y}_r) - \frac{1}{r_1} \tilde{\varpi}_1^T \dot{\tilde{\varpi}}_1. \end{aligned} \tag{17}$$

Using Young’s inequality to deal with terms $e_1 \eta_2$ and $e_1 \epsilon_1$, the time derivative \dot{V}_1 of V_1 can be rewritten

$$\begin{aligned} \dot{V}_1 \leq & e_1(-A_{2,1} e_1^{2q-1} + A_{2,1} e_1^{2q-1} \\ & + e_1 + e_2 + \alpha_1 - \dot{y}_r + \tilde{\varpi}_1^T \varphi_1(x)) \\ & + \frac{1}{2} \eta_2^2 + \frac{1}{2} \epsilon_1^2 + \tilde{\varpi}_1^T \left(-\frac{1}{r_1} \dot{\tilde{\varpi}}_1 + e_1 \varphi_1(x) \right) \end{aligned} \tag{18}$$

At this point, the virtual controller α_1 and the adaptive law $\dot{\hat{\varpi}}_1$ are deduced

$$\alpha_1 = -A_{1,1} e_1^{2p-1} - A_{2,1} e_1^{2q-1} - \hat{\varpi}_1^T \varphi_1(x) - e_1 + \dot{y}_r, \tag{19}$$

$$\dot{\hat{\varpi}}_1 = r_1 e_1 \varphi_1(x) - R_1 \hat{\varpi}_1, \tag{20}$$

where $A_{1,1}, A_{2,1}, p, q, R_1$, and r_1 are all design parameters that simultaneously satisfy $A_{1,1}, A_{2,1}, R_1, r_1 > 0, 0 < p < 1, q > 1$.

By inserting the virtual controller α_1 and the adaptive law $\dot{\hat{\omega}}_1$ into (18), the final form of \dot{V}_1 can be written as

$$\begin{aligned} \dot{V}_1 \leq & e_1 e_2 - A_{1,1} e_1^{2p} - A_{2,1} e_1^{2q} + \frac{R_1}{r_1} \tilde{\omega}_1^T \hat{\omega}_1 \\ & + \frac{1}{2} \epsilon_1^2 + \frac{1}{2} \eta_2^2 \end{aligned} \tag{21}$$

In order to avoid the ‘‘complex explosion’’ problem, a first-order linear filter of the following form is introduced

$$\delta_2 \dot{\omega}_2 + \omega_2 = \alpha_1, \tag{22}$$

where $\omega_2(0) = \alpha_1(0)$ and $\delta_2 > 0$ is constant.

Substituting $\eta_2 = \omega_2 - \alpha_1$ into (22), $\dot{\omega}_2 = -\frac{\eta_2}{\delta_2}$ can be obtained after simplifying. Due to $\dot{\eta}_2 = \dot{\omega}_2 - \dot{\alpha}_1$, one can deduce

$$\dot{\eta}_2 = -\frac{\eta_2}{\delta_2} + Q_2, \tag{23}$$

where $Q_2 = -\dot{\alpha}_1 = (2p - 1)A_{1,1}e_1^{2p-2} + (2q - 1)A_{2,1}e_1^{2q-2} + \dot{e}_1 - \ddot{y}_r + \hat{\omega}_1^T \varphi_1(x_1) + \hat{\omega}_1^T \frac{\partial \varphi_1(x_1)}{\partial x_1} \dot{x}_1$.

Remark 2 The traditional backstepping method requires repeated differentiation of the virtual controller at each step, therefore, as the system order increases, the computational workload will grow exponentially. It is shown that when the system order is greater than 3, the actual controller structure will be extremely complex in the backstepping recursive process [34, 35]. The dynamic surface technique introduces a first-order filter based on the traditional backstepping method to replace the first-order derivative of the virtual controller so that simple algebraic operations replaced the original complex differential operations. When the system order is relatively low, the complexity of the two methods is not obvious. With the increase of the order, the advantage of dynamic surface technique in reducing the computation redundancy becomes more obvious. Swaroop et al. [36] give a more detailed comparison of the two methods.

Step i ($2 \leq i \leq n - 1$): According to the coordinate transformation of the i -th step and system (1), the following equation can be obtained:

$$\dot{e}_i = e_{i+1} + \eta_{i+1} + \alpha_i + \epsilon_i + \tilde{\omega}_i^T \varphi_i(x) + \hat{\omega}_i^T \varphi_i(x) - \dot{\omega}_i, \tag{24}$$

where $\epsilon_i > 0$ is the approximation error of FLSSs.

Choose the Lyapunov function candidate with $r_i > 0$

$$V_i = V_{i-1} + \frac{1}{2} e_i^2 + \frac{1}{2} \eta_i^2 + \frac{1}{2r_i} \tilde{\omega}_i^T \hat{\omega}_i. \tag{25}$$

It follows from (24) and (25) that

$$\begin{aligned} \dot{V}_i = & \dot{V}_{i-1} + e_i(e_{i+1} + \eta_{i+1} + \alpha_i + \epsilon_i - \dot{\omega}_i + \tilde{\omega}_i^T \varphi_i(x) \\ & + \hat{\omega}_i^T \varphi_i(x)) + \eta_i(-\frac{\eta_i}{\delta_i} + Q_i) - \frac{1}{r_i} \tilde{\omega}_i^T \dot{\hat{\omega}}_i \end{aligned} \tag{26}$$

According to Lemma 1, the following inequalities hold

$$e_i \eta_{i+1} \leq \frac{1}{2} e_i^2 + \frac{1}{2} \eta_{i+1}^2, \tag{27}$$

$$e_i \epsilon_i \leq \frac{1}{2} e_i^2 + \frac{1}{2} \epsilon_i^2, \tag{28}$$

$$\eta_i Q_i \leq \frac{1}{2k} \eta_i^2 Q_i^2 + \frac{1}{2} k, \tag{29}$$

where $k > 0$.

Substituting (27), (28), and (29) into (26) produces

$$\begin{aligned} \dot{V}_i = & \dot{V}_{i-1} - e_{i-1} e_i - \frac{1}{2} \eta_i^2 + e_i(e_{i-1} + e_{i+1} \\ & + \alpha_i - \dot{\omega}_i + e_i + \hat{\omega}_i^T \varphi_i(x)) \\ & - \eta_i^2 \left(\frac{1}{\delta_i} - \frac{1}{2k} Q_i^2 - \frac{1}{2} \right) + \frac{1}{2} \epsilon_i^2 + \frac{1}{2} k \\ & + \frac{1}{2} \eta_{i+1}^2 + \tilde{\omega}_i^T \left(-\frac{1}{r_i} \dot{\hat{\omega}}_i + e_i \varphi_i(x) \right) \end{aligned} \tag{30}$$

Therefore, the virtual controller α_i and the adaptive law $\dot{\hat{\omega}}_i$ are constructed

$$\alpha_i = -A_{1,i} e_i^{2p-1} - A_{2,i} e_i^{2q-1} - \hat{\omega}_i^T \varphi_i(x) - e_{i-1} - e_i + \dot{\omega}_i, \tag{31}$$

$$\dot{\hat{\omega}}_i = r_i e_i \varphi_i(x) - R_i \hat{\omega}_i, \tag{32}$$

where $A_{1,i}$ and $A_{2,i}$ are design parameters that simultaneously satisfy $A_{1,i} > 0, A_{2,i} > 0$.

Substituting the above two equations into (30), \dot{V}_i can be written as

$$\begin{aligned} \dot{V}_i \leq & e_i e_{i+1} - \sum_{j=1}^i A_{1,j} e_j^{2p} - \sum_{j=1}^i A_{2,j} e_j^{2q} - \sum_{j=2}^i \eta_j^2 \left(\frac{1}{\delta_j} - \frac{1}{2k} Q_j^2 \right. \\ & \left. - \frac{1}{2} \right) + \sum_{j=1}^i \frac{1}{2} \epsilon_j^2 + \sum_{j=1}^i \frac{R_j}{r_j} \tilde{\omega}_j^T \hat{\omega}_j + \frac{1}{2} \eta_{i+1}^2 + \frac{i-1}{2} k \end{aligned} \tag{33}$$

Construct the filter according to the method in step 1

$$\delta_{i+1} \dot{\omega}_{i+1} + \omega_{i+1} = \alpha_i, \tag{34}$$

where $\omega_{i+1}(0) = \alpha_i(0)$ and $\delta_{i+1} > 0$ is constant.

Substituting $\eta_{i+1} = \omega_{i+1} - \alpha_i$ into (34), $\dot{\omega}_{i+1} = -\frac{\eta_{i+1}}{\delta_{i+1}}$ can be obtained after simplifying. Due to $\dot{\eta}_{i+1} = \dot{\omega}_{i+1} - \dot{\alpha}_i$, one can deduce

$$\dot{\eta}_{i+1} = -\frac{\eta_{i+1}}{\delta_{i+1}} + Q_{i+1}, \tag{35}$$

where $Q_{i+1} = -\dot{\alpha}_i = (2p - 1)A_{1,i}e_i^{2p-2} + (2q - 1)A_{2,i}e_i^{2q-2} + \dot{e}_{i-1} + \dot{e}_i + \hat{\omega}_i^T \varphi_i(x_i) + \hat{\omega}_i^T \frac{\partial \varphi_i(x_i)}{\partial x_i} \dot{x}_i + \frac{\eta_i}{\delta_i}$.

Step n: In the light of coordinate transformations and nonlinear system (1), \dot{e}_n can be written as

$$\dot{e}_n = u + f_n(x) + \zeta(t - T_0)\tau(x, u) - \dot{\omega}_n. \tag{36}$$

Define the following augmented Lyapunov function with $r_n > 0$ as

$$V_n = V_{n-1} + \frac{1}{2}e_n^2 + \frac{1}{2}\eta_n^2 + \frac{1}{2r_n}\tilde{\omega}_n^T\tilde{\omega}_n. \tag{37}$$

Combining (36) and (37) gets the time derivative \dot{V}_n of V_n

$$\begin{aligned} \dot{V}_n = & \dot{V}_{n-1} + e_n(u + f_n(x) + \zeta(t - T_0)\tau(x, u) \\ & - \dot{\omega}_n) + \eta_n(-\frac{\eta_n}{\delta_n} + Q_n) - \frac{1}{r_n}\tilde{\omega}_n^T\dot{\tilde{\omega}}_n \end{aligned} \tag{38}$$

According to (38), $\zeta(t - T_0)\tau(x, u)$ is the failure encountered by the system, $\tau(x, u)$ represents the non-affine nonlinear fault function involving system state and controller output and $\zeta(t - T_0)$ refers to the homologous time profile of the fault that occurs at some unknown time. In order to improve the fault-tolerance of the system and ensure the normal operation of the system, it is necessary to use the idea of fault-tolerance to design the controller and the adaptive law. The noteworthy point is that this paper is based on the idea of passive fault-tolerance, the adaptive law is designed to replace the fault detection and isolation module. The adaptive law evaluates the fault level and feeds the evaluation results back to the fault-tolerant controller. Then, under the action of fault-tolerant controller, the effects and changes of system non-dynamics caused by faults are weakened.

In order to design an adaptive law and a controller with fault-tolerance, the following processes are required.

Consider $f_n(x)$ and $\zeta(t - T_0)\tau(x, u)$ as a whole, and use the knowledge of Assumption 2 to deal with the faults, that is

$$e_n(f_n(x) + \zeta(t - T_0)\tau(x, u)) \leq |e_n| \|\bar{h}(x, u)\|. \tag{39}$$

The final result is obtained by using Young's inequality

$$|e_n| \|\bar{h}(x, u)\| \leq \frac{1}{2b}e_n^2\bar{h}^2(x, u) + \frac{1}{2}b. \tag{40}$$

Let $h(x, u) = \frac{1}{2b}e_n\bar{h}^2(x, u)$, and use FLSs to process $h(x, u)$, the following inequality holds

$$\begin{aligned} |e_n| \|\bar{h}(x, u)\| & \leq e_n h(x, u) + \frac{1}{2}b \\ & \leq e_n(\epsilon_n + \tilde{\omega}_n^T \varphi_n(x) + \hat{\omega}_n^T \varphi_n(x)) + \frac{1}{2}b, \end{aligned} \tag{41}$$

where $b > 0$ and $\epsilon_n > 0$ are the design parameter and the approximation error of FLSs.

At this point, fault handling is complete.

Using Young's inequality deals with the term $e_n\epsilon_n$ and the term $\eta_n Q_n$

$$e_n\epsilon_n \leq \frac{1}{2}e_n^2 + \frac{1}{2}\epsilon_n^2, \tag{42}$$

$$\eta_n Q_n \leq \frac{1}{2k}\eta_n^2 Q_n^2 + \frac{1}{2}k. \tag{43}$$

Substituting (39), (41), (42), and (43) into (38), the following inequality is derived:

$$\begin{aligned} \dot{V}_n \leq & \dot{V}_{n-1} - e_{n-1}e_n - \frac{1}{2}\eta_n^2 + e_n(u + \hat{\omega}_n^T \varphi_n(x) + \frac{1}{2}e_n \\ & - e_{n-1} - \dot{\omega}_n) - \eta_n^2(\frac{1}{\delta_n} - \frac{1}{2k}Q_n^2 - \frac{1}{2}) + \frac{1}{2}\epsilon_n^2 + \frac{1}{2}k \\ & + \frac{1}{2}b + \tilde{\omega}_n^T(-\frac{1}{r_n}\dot{\tilde{\omega}}_n + e_n\varphi_n(x)) \end{aligned} \tag{44}$$

So the required actual controller u and adaptive law $\dot{\tilde{\omega}}_n$ are obtained

$$u = -A_{1,n}e_n^{2p-1} - A_{2,n}e_n^{2q-1} - \hat{\omega}_n^T \varphi_n(x) - e_{n-1} - \frac{1}{2}e_n + \dot{\omega}_n, \tag{45}$$

$$\dot{\tilde{\omega}}_n = r_n e_n \varphi_n(x) - R_n \hat{\omega}_n, \tag{46}$$

where $A_{1,n}$ and $A_{2,n}$ are design parameters that simultaneously satisfy $A_{1,n} > 0, A_{2,n} > 0$.

Substituting (45) and (46) into (44), \dot{V}_n can be rewritten as

$$\begin{aligned} \dot{V}_n \leq & -\sum_{j=1}^n A_{1,j}e_j^{2p} - \sum_{j=1}^n A_{2,j}e_j^{2q} + \sum_{j=1}^n \frac{1}{2}\epsilon_j \\ & + \sum_{j=1}^n \frac{R_j}{r_j}\tilde{\omega}_j^T\dot{\tilde{\omega}}_j \\ & - \sum_{j=2}^n \eta_j^2\left(\frac{1}{\delta_j} - \frac{1}{2k}Q_j^2 - \frac{1}{2}\right) + \frac{n-1}{2}k + \frac{1}{2}b \end{aligned} \tag{47}$$

Based on the above discussions, the block diagram of the design procedure for the proposed controller is shown in Fig. 1.

Remark 3 The most significant parts of fault-tolerant control policies in this paper are the design of the fixed-time fault-tolerant controller. The non-affine nonlinear

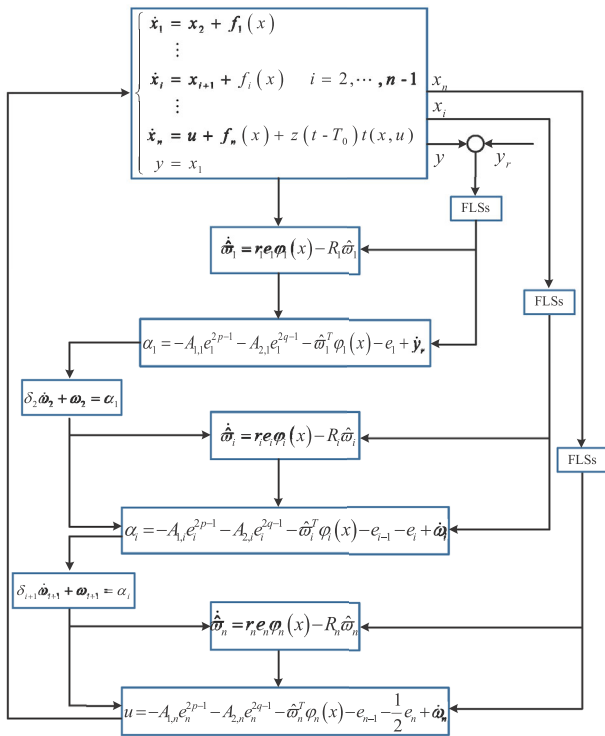


Fig. 1 The block diagram of the design procedure for the proposed controller

faults involving system state and controller output are transformed into compound nonlinear function which can be approximated by fuzzy logic systems. Based on the dynamic surface technique and Lyapunov fixed-time stability criterion, the adaptive fuzzy fixed-time controller and the adaptive law are designed, where the adaptive law is used to estimate the fault level and feed the results back to the fault-tolerant controller, which performs control actions to weaken the influence of faults on the system.

3.2 Stability Analysis

According to the design process in Part 3.1, the following theorem is summarized.

Theorem 1 Consider the uncertain nonlinear plant (1) subjected to actuator faults that belong to the non-affine fault type. The dynamic surface control technique combined with the backstepping method avoids the repeated derivation of the virtual controller α_i , where $i = 1, 2, \dots, n - 1$. Under Assumptions 1 – 2, the fault-tolerant controller (45), with the intermediate virtual controllers (19), (31), and adaptive laws (20), (32), and

(46) guarantee that all the signals in the closed-loop system are semi-globally uniformly ultimately bounded in probability. The output y of the control system can track the desired signal y_r with a high enough accuracy.

The proof of Theorem 1 is as follows.

Proof To make the above control scheme meet the fixed-time stability condition of Lemma 3, we need to do the following processing for (47).

First of all, the term $\sum_{j=1}^n \frac{R_j}{r_j} \tilde{\omega}_j^T \hat{\omega}_j$ is handled. According to $\tilde{\omega} = \omega^* - \hat{\omega}$ and Young’s inequality, $\tilde{\omega}^T \hat{\omega} = \tilde{\omega}^T (\omega^* - \tilde{\omega})$ is deduced, and then the following inequality holds

$$\sum_{j=1}^n \frac{R_j}{r_j} \tilde{\omega}_j^T \hat{\omega}_j \leq \sum_{j=1}^n \frac{R_j}{2r_j} \omega_j^{*T} \omega_j^* - \sum_{j=1}^n \frac{R_j}{2r_j} \tilde{\omega}_j^T \tilde{\omega}_j. \tag{48}$$

Replacing the term $\sum_{j=1}^n \frac{R_j}{r_j} \tilde{\omega}_j^T \hat{\omega}_j$ in (47) with (48) has

$$\begin{aligned} \dot{V}_n \leq & - \sum_{j=1}^n A_{1,j} e_j^{2p} - \sum_{j=1}^n A_{2,j} e_j^{2q} - \sum_{j=1}^n \frac{R_j}{2r_j} \tilde{\omega}_j^T \tilde{\omega}_j + \frac{n-1}{2} k + \frac{1}{2} b \\ & - \sum_{j=2}^n \eta_j^2 \left(\frac{1}{\delta_j} - \frac{1}{2k} Q_j^2 - \frac{1}{2} \right) \\ & + \sum_{j=1}^n \frac{R_j}{2r_j} \omega_j^{*T} \omega_j^* + \sum_{j=1}^n \frac{1}{2} \epsilon_j \end{aligned} \tag{49}$$

Let $a = \min\{A_{1,1}, \dots, A_{1,n}, A_{2,1}, \dots, A_{2,n}, \frac{1}{\delta_2} - \frac{Q_2^2}{2k} - \frac{1}{2}, \dots, \frac{1}{\delta_n} - \frac{Q_n^2}{2k} - \frac{1}{2}, \frac{R_1}{2}, \dots, \frac{R_n}{2}\}$, and $W_1 = \sum_{j=1}^n \frac{R_j}{2r_j} \omega_j^{*T} \omega_j^* + \sum_{j=1}^n \frac{1}{2} \epsilon_j + \frac{n-1}{2} k + \frac{1}{2} b$, the inequality (49) can be simplified into the following form

$$\begin{aligned} \dot{V}_n \leq & -a \sum_{j=1}^n e_j^{2p} - a \sum_{j=1}^n e_j^{2q} \\ & - a \sum_{j=2}^n \eta_j^2 - a \sum_{j=1}^n \frac{1}{r_j} \tilde{\omega}_j^T \tilde{\omega}_j + W_1 \end{aligned} \tag{50}$$

Second, use Lemma 2 to deal with terms $a \sum_{j=1}^n e_j^{2p}$ and $a \sum_{j=1}^n e_j^{2q}$

$$a \sum_{j=1}^n e_j^{2p} = 2^p a \sum_{j=1}^n \left(\frac{e_j^2}{2} \right)^p \geq 2^p a \left(\sum_{j=1}^n \frac{e_j^2}{2} \right)^p, \tag{51}$$

$$a \sum_{j=1}^n e_j^{2q} = 2^q a \sum_{j=1}^n \left(\frac{e_j^2}{2} \right)^q \geq 2^q n^{1-q} a \left(\sum_{j=1}^n \frac{e_j^2}{2} \right)^q. \tag{52}$$

Substituting (51) and (52) into (50) gives

$$\begin{aligned}
 \dot{V}_n \leq & -2^p a \left(\sum_{j=1}^n \frac{e_j^2}{2} \right)^p - 2^p n^{1-q} a \left(\sum_{j=1}^n \frac{e_j^2}{2} \right)^q \\
 & - a \left(\sum_{j=2}^n \frac{1}{2} \eta_j^2 \right)^p - a \sum_{j=2}^n \left(\frac{1}{2} \eta_j^2 \right)^q \\
 & - a \left(\sum_{j=1}^n \frac{1}{2r_j} \tilde{\omega}_j^T \tilde{\omega}_j \right)^p \\
 & - a \sum_{j=1}^n \left(\frac{1}{2r_j} \tilde{\omega}_j^T \tilde{\omega}_j \right)^q + a \left(\sum_{j=1}^n \frac{1}{2r_j} \tilde{\omega}_j^T \tilde{\omega}_j \right)^p \\
 & + a \left(\sum_{j=2}^n \frac{1}{2} \eta_j^2 \right)^p + a \sum_{j=2}^n \left(\frac{1}{2} \eta_j^2 \right)^q - a \sum_{j=2}^n \frac{1}{2} \eta_j^2 \\
 & + a \sum_{j=1}^n \left(\frac{1}{2r_j} \tilde{\omega}_j^T \tilde{\omega}_j \right)^q \\
 & - a \sum_{j=1}^n \frac{1}{2r_j} \tilde{\omega}_j^T \tilde{\omega}_j \\
 & - a \sum_{j=2}^n \frac{1}{2} \eta_j^2 - a \sum_{j=1}^n \frac{1}{2r_j} \tilde{\omega}_j^T \tilde{\omega}_j + W_1
 \end{aligned} \tag{53}$$

In the light of Young's Inequality, one get $\left(\sum_{j=2}^n \frac{1}{2} \eta_j^2 \right)^p \leq (1-p)p^{\frac{p}{1-p}} + \sum_{j=2}^n \frac{1}{2} \eta_j^2$ and $\left(\sum_{j=1}^n \frac{1}{2r_j} \tilde{\omega}_j^T \tilde{\omega}_j \right)^p \leq (1-p)p^{\frac{p}{1-p}} + \sum_{j=1}^n \frac{1}{2r_j} \tilde{\omega}_j^T \tilde{\omega}_j$.

Therefore, (53) can be rewritten as

$$\begin{aligned}
 \dot{V}_n \leq & -c \left(\sum_{j=1}^n \frac{e_j^2}{2} \right)^p - c \left(\sum_{j=1}^n \frac{e_j^2}{2} \right)^q \\
 & - c \left(\sum_{j=2}^n \frac{1}{2} \eta_j^2 \right)^p - c \left(\sum_{j=1}^n \frac{1}{2r_j} \tilde{\omega}_j^T \tilde{\omega}_j \right)^p \\
 & - c \left(\sum_{j=1}^n \frac{1}{2r_j} \tilde{\omega}_j^T \tilde{\omega}_j \right)^q \\
 & - c \left(\sum_{j=2}^n \frac{1}{2} \eta_j^2 \right)^q + c \sum_{j=2}^n \left(\frac{1}{2} \eta_j^2 \right)^q - c \sum_{j=2}^n \frac{1}{2} \eta_j^2 \\
 & + c \sum_{j=1}^n \left(\frac{1}{2r_j} \tilde{\omega}_j^T \tilde{\omega}_j \right)^q - c \sum_{j=1}^n \frac{1}{2r_j} \tilde{\omega}_j^T \tilde{\omega}_j + W_2
 \end{aligned} \tag{54}$$

where $c = \min\{2^p a, 2^q n^{1-q} a, a\}$ and $W_2 = 2(1-p)p^{\frac{p}{1-p}} + W_1$.

If the conditions $q > 1$ is met, it can be divided into four situations to discuss.

Case 1: If $\tilde{\omega}_j^T \tilde{\omega}_j < 2r_j$ and $\eta_j^2 < 2$, the following inequality holds

$$c \sum_{j=1}^n \left(\frac{1}{2r_j} \tilde{\omega}_j^T \tilde{\omega}_j \right)^q - c \sum_{j=1}^n \frac{1}{2r_j} \tilde{\omega}_j^T \tilde{\omega}_j < 0, \tag{55}$$

$$c \sum_{j=2}^n \left(\frac{1}{2} \eta_j^2 \right)^q - c \sum_{j=2}^n \frac{1}{2} \eta_j^2 < 0. \tag{56}$$

At this point, combining Lemma 2, (56) can be rewritten as

$$\begin{aligned}
 \dot{V}_n \leq & -3^{1-q} c \left(\sum_{j=1}^n \frac{e_j^2}{2} + \sum_{j=2}^n \frac{1}{2} \eta_j^2 + \sum_{j=1}^n \frac{1}{2r_j} \tilde{\omega}_j^T \tilde{\omega}_j \right)^q \\
 & - c \left(\sum_{j=1}^n \frac{e_j^2}{2} + \sum_{j=2}^n \frac{1}{2} \eta_j^2 + \sum_{j=1}^n \frac{1}{2r_j} \tilde{\omega}_j^T \tilde{\omega}_j \right)^p + W_2 \\
 \leq & -CV_n^p - SV_n^q + W_2
 \end{aligned} \tag{57}$$

Case 2: If $\tilde{\omega}_j^T \tilde{\omega}_j < 2r_j$ and $\eta_j^2 > 2$, the following inequality holds

$$c \sum_{j=1}^n \left(\frac{1}{2r_j} \tilde{\omega}_j^T \tilde{\omega}_j \right)^q - c \sum_{j=1}^n \frac{1}{2r_j} \tilde{\omega}_j^T \tilde{\omega}_j < 0, \tag{58}$$

$$c \sum_{j=2}^n \left(\frac{1}{2} \eta_j^2 \right)^q - c \sum_{j=2}^n \frac{1}{2} \eta_j^2 > 0. \tag{59}$$

At this point, (56) can be rewritten as

$$\dot{V}_n \leq -CV_n^p - SV_n^q + W_3. \tag{60}$$

Case 3: If $\tilde{\omega}_j^T \tilde{\omega}_j > 2r_j$ and $\eta_j^2 < 2$, the following inequality holds

$$c \sum_{j=1}^n \left(\frac{1}{2r_j} \tilde{\omega}_j^T \tilde{\omega}_j \right)^q - c \sum_{j=1}^n \frac{1}{2r_j} \tilde{\omega}_j^T \tilde{\omega}_j > 0. \tag{61}$$

$$c \sum_{j=2}^n \left(\frac{1}{2} \eta_j^2 \right)^q - c \sum_{j=2}^n \frac{1}{2} \eta_j^2 < 0. \tag{62}$$

In the same way,

$$\dot{V}_n \leq -CV_n^p - SV_n^q + W_4. \tag{63}$$

Case 4: If $\tilde{\omega}_j^T \tilde{\omega}_j > 2r_j$ and $\eta_j^2 > 2$, the following inequality holds

$$c \sum_{j=1}^n \left(\frac{1}{2r_j} \tilde{\omega}_j^T \tilde{\omega}_j \right)^q - c \sum_{j=1}^n \frac{1}{2r_j} \tilde{\omega}_j^T \tilde{\omega}_j > 0, \tag{64}$$

$$c \sum_{j=2}^n \left(\frac{1}{2} \eta_j^2 \right)^q - c \sum_{j=2}^n \frac{1}{2} \eta_j^2 > 0. \tag{65}$$

Similarly,

$$\dot{V}_n \leq -CV_n^p - SV_n^q + W_5, \tag{66}$$

where $C = c$, $S = 3^{1-q}c$, $W_3 = W_2 + c \sum_{j=2}^n \left(\frac{1}{2}\eta_j^2\right)^q - c \sum_{j=2}^n \frac{1}{2}\eta_j^2$, $W_4 = W_2 + c \sum_{j=1}^n \left(\frac{1}{2r_j}\tilde{\omega}_j^T\tilde{\omega}_j\right)^q - c \sum_{j=1}^n \frac{1}{2r_j}\tilde{\omega}_j^T\tilde{\omega}_j$, and $W_5 = W_2 + c \sum_{j=1}^n \left(\frac{1}{2r_j}\tilde{\omega}_j^T\tilde{\omega}_j\right)^q - c \sum_{j=1}^n \frac{1}{2r_j}\tilde{\omega}_j^T\tilde{\omega}_j + c \sum_{j=2}^n \left(\frac{1}{2}\eta_j^2\right)^q - c \sum_{j=2}^n \frac{1}{2}\eta_j^2$.

Therefore, based on the above analysis, it is clear that the proposed control scheme satisfies Lemma 3 and Theorem 1 holds.

Remark 4 The control performance of the system depends on many design parameters. It can be seen from the stability analysis that the parameters $A_{1,i}$, $A_{2,i}$, r_i , and R_i can adjust the convergence error and convergence accuracy at the same time. By selecting larger $A_{2,i}$, smaller R_i as well as appropriate $A_{1,i}$, r_i , the convergence speed can be improved and the final error can be reduced. In addition, the exponents p and q determine the boundary of the convergence time and influence the convergence accuracy. Choosing suitable exponents can reduce the convergence time and improve the convergence accuracy.

4 Simulation Studies

Two simulation examples are used to verify the effectiveness of the above designed fault-tolerant control scheme.

Example 1 (Numerical Simulation): Consider the following second-order nonstrict nonlinear systems with non-affine faults

$$\begin{cases} \dot{x}_1 = x_2 + f_1(x) \\ \dot{x}_2 = u + f_2(x) + \zeta(t - T_0)\tau(x, u), \\ y = x_1 \end{cases} \quad (67)$$

where $f_1(x) = 0$, $f_2(x) = x_2 \sin(x_1)e^{-(1+2x_1x_2)}$. We assume that the ideal reference signal is $y_r = 0.5\sin(t)$. The approximation error of the system is $e = y - y_r$. In this paper, we consider two types of faults: incipient fault and abrupt fault. From formulas (2) and (3), it can be seen that $\zeta(t - T_0) = 0, (T_0 < 10)$ and $\zeta(t - T_0) = 1 - e^{-\varrho(t-T_0)}, (T_0 \geq 10)$, where T_0 is the time of the fault occurred. If ϱ is a bounded constant (this simulation assumes $\varrho = 23$), the fault considered is an incipient fault. If ϱ approaches infinity, the fault considered is abrupt fault. The fault function is defined as $\tau(x, u) = 5(x_1x_2 + \sin(u)) + 10$.

In the simulation study, fuzzy if-then rules are chosen as follows:

- Υ^1 : if x_1^1 is Ψ_1^1 and x_2^1 is Ψ_2^1 , then y is Φ^1 ;
- Υ^2 : if x_1^2 is Ψ_1^2 and x_2^2 is Ψ_2^2 , then y is Φ^2 ;

- Υ^3 : if x_1^3 is Ψ_1^3 and x_2^3 is Ψ_2^3 , then y is Φ^3 ;
- Υ^4 : if x_1^4 is Ψ_1^4 and x_2^4 is Ψ_2^4 , then y is Φ^4 ;
- Υ^5 : if x_1^5 is Ψ_1^5 and x_2^5 is Ψ_2^5 , then y is Φ^5 ;

where fuzzy sets are chosen as $\Psi_1^1 = (NL)$, $\Psi_2^1 = (NL)$, $\Psi_1^2 = (NS)$, $\Psi_2^2 = (NS)$, $\Psi_1^3 = (ZE)$, $\Psi_2^3 = (ZE)$, $\Psi_1^4 = (PS)$, $\Psi_2^4 = (PS)$, $\Psi_1^5 = (PL)$, $\Psi_2^5 = (PL)$, which are defined over the interval $[-2, 2]$ for variables x_1^k and x_2^k , respectively. NL, NS, ZE, PS and PL denote negative large, negative small, zero, positive small, positive large, respectively. Their center points are selected as $-2, -1, 0, 1, 2$, respectively. The fuzzy membership functions for each fuzzy set are chosen as Gaussian-shaped membership functions, and they are given as follows:

$$\mu\Psi_i^k(x_i^k) = \exp\left[-\frac{(x_i^k + 3 - k)^2}{4^2}\right] \quad i = 1, 2 \quad k = 1, 2, 3, 4, 5. \quad (68)$$

According to the controller design flow in Sect. 3, the fixed-time fault-tolerant controllers and adaptive laws designed for the second-order system (67) are shown below.

$$\alpha_1 = -A_{1,1}e_1^{2p-1} - A_{2,1}e_1^{2q-1} - \frac{1}{2}e_1 + \dot{y}_r, \quad (69)$$

$$u = -A_{1,2}e_2^{2p-1} - A_{2,2}e_2^{2q-1} - \frac{1}{2}e_2 - e_1 - \tilde{\omega}_2^T\varphi_2(x_2) + \dot{\omega}, \quad (70)$$

$$\dot{\hat{\theta}}_1 = 0, \quad (71)$$

$$\dot{\hat{\theta}}_2 = r_2e_2\varphi_2(x_2) - R_2\hat{\omega}_2. \quad (72)$$

In order to make the simulation results more convincing, we compare the adaptive fuzzy fixed-time fault-tolerant controller proposed in this paper with the adaptive fuzzy finite-time fault-tolerant controller under the condition that the considered system and related parameters are consistent. The relevant parameters are chosen as $A_{1,1} = 1$, $A_{2,1} = 50$, $A_{1,2} = 30$, $A_{2,2} = 100$, $p = 0.9$, $q = 1.5$, $r_2 = 2$, $R_2 = 0.5$, $\delta_2 = 0.01$. We choose 0.3 and -0.1 as the initial conditions of state variables x_1 and x_2 . The initial value $\hat{\theta}(0)$ of $\hat{\theta}$ is set to $[0, 0, 0, 0, 0]^T$. The above parameter values are used whether the system suffers from the incipient fault or the abrupt fault. The simulation results are presented in Figs. 2 and 3. Figure 2 shows the simulation comparison results of the two scheme when the system suffers from the incipient fault. Figure 2a is the state variable trajectories of the system under the control of the two schemes. The tracking errors of the system are shown in Fig. 2b. Figure 2c and d displays the output trajectories of the system and the waveforms of the controller under two schemes, respectively. Figure 3 shows the simulation

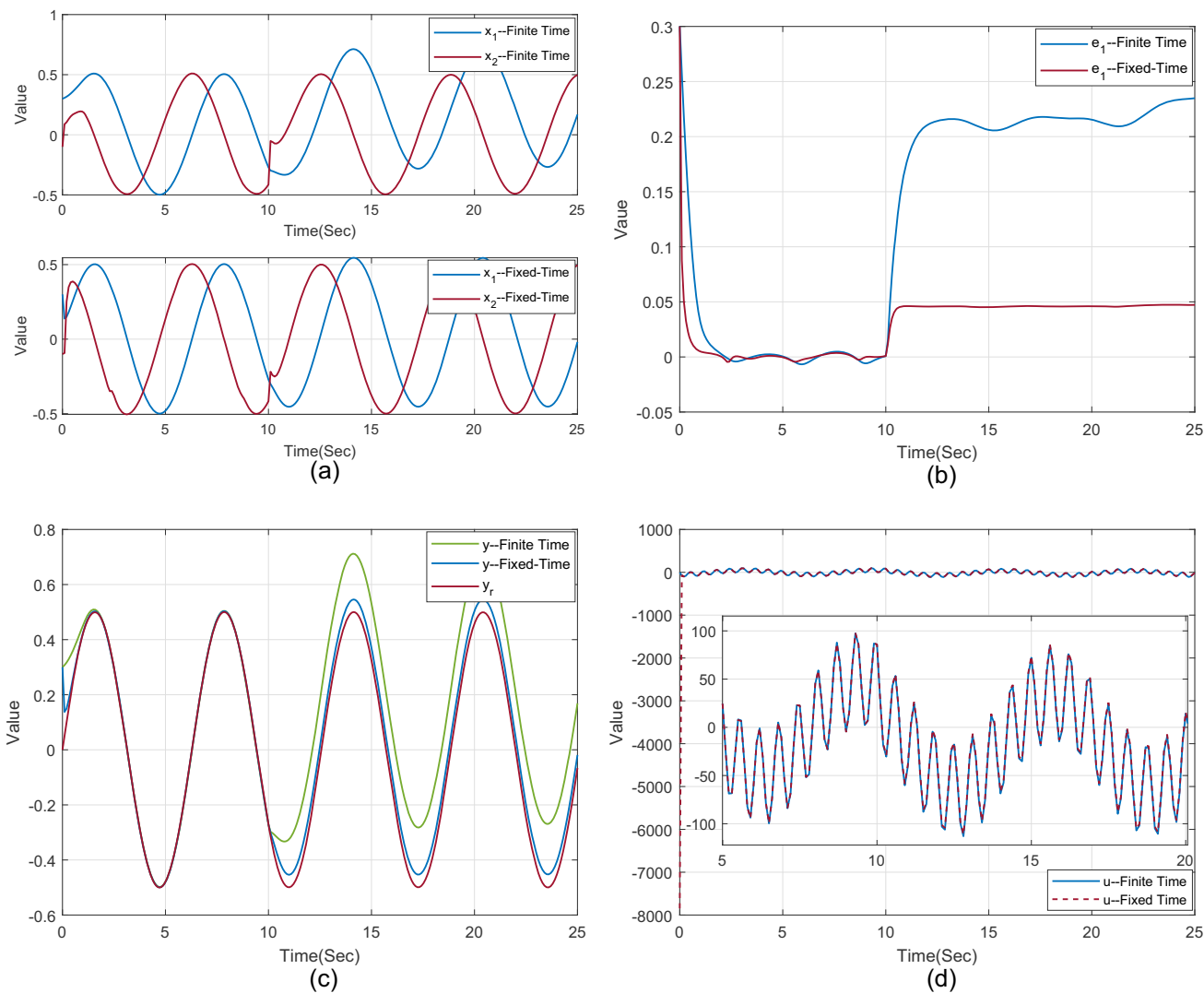


Fig. 2 **a** Comparison trajectories of x_1 and x_2 under incipient fault, **b** comparison trajectories of e_1 under incipient fault, **c** comparison trajectories of y and y_r under incipient fault, **d** Comparison trajectories of u under incipient fault

comparing results of the two scheme when the system suffers from the abrupt fault. Correspondingly, Fig. 3a–d represents the state variable trajectories, tracking error trajectories, system output trajectories, and controller waveforms for the considered system under the control of the two schemes, respectively.

From Figs. 2 and 3, it is clear that the fixed-time fault-tolerant control scheme proposed in this paper is superior to the finite-time fault-tolerant control scheme both in terms of convergence speed and control accuracy. When the fault does not occur, the difference is not significant in tracking accuracy between the fixed-time fault-tolerant control scheme and the finite-time fault-tolerant control scheme. When the fault occurs, the tracking accuracy of the system under the fixed-time fault-tolerant control scheme decreases but still meets the requirements of the

system. However, the tracking accuracy of the system under the finite-time fault-tolerant control scheme shows the phenomenon of divergence as time increased.

Example 2 (Model Simulation): With reference to the robotic manipulator system proposed in Wang et al. [37], we verify the control effect of the control strategy proposed above. The dynamic equation of the robotic manipulator system is shown as follows:

$$\begin{cases} D\ddot{q} + B\dot{q} + Mgl \sin(q) = \tau \\ M_m \dot{\tau} + H_m \tau = u - K_m \dot{q} \end{cases}, \tag{73}$$

where the physical significance of q , \dot{q} and \ddot{q} are the angle, angular velocity and angular acceleration of the link, respectively. The rotation inertia of the servo motor, the mass of the link, the gravitational acceleration, and the

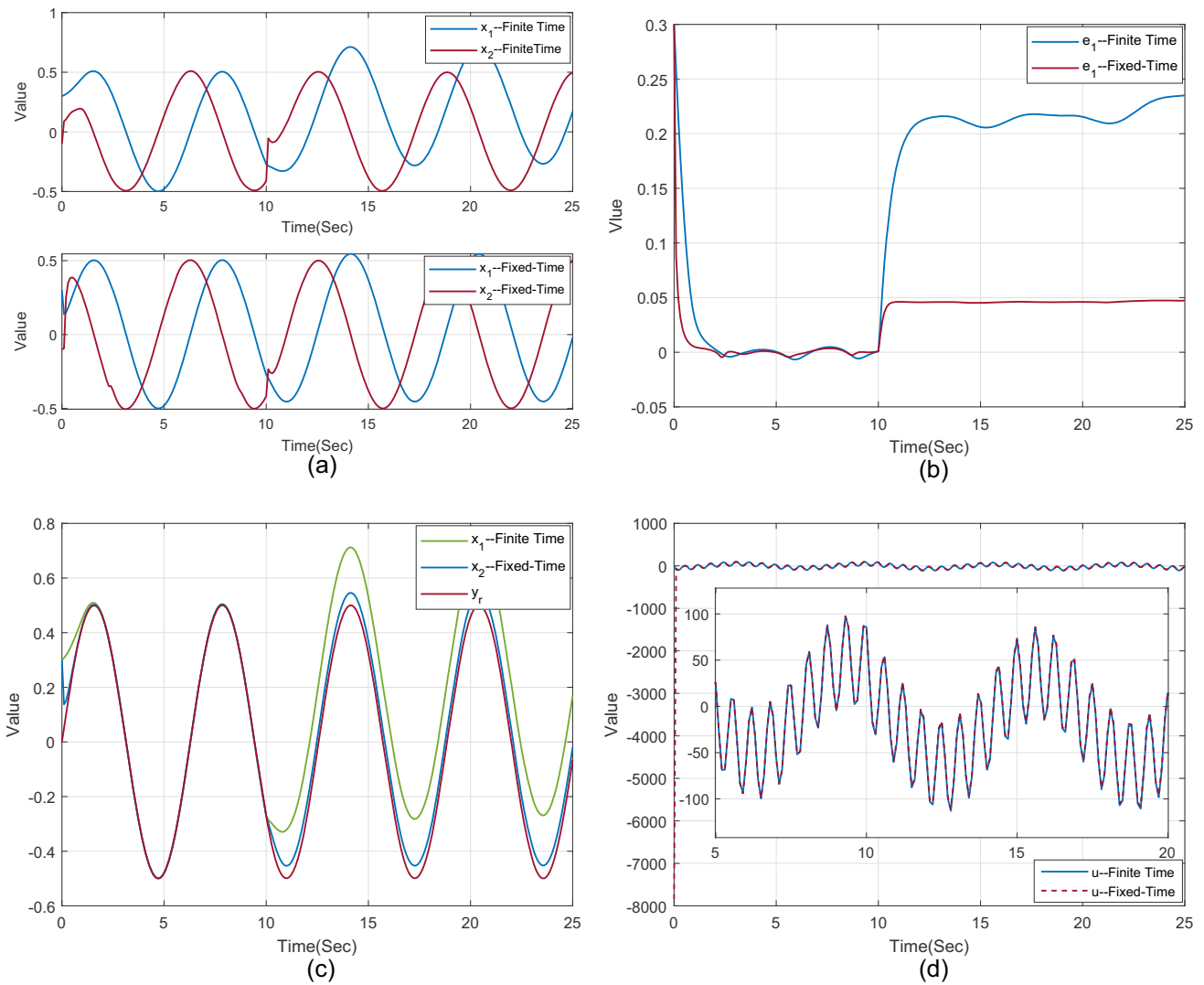


Fig. 3 **a** Comparison trajectories of x_1 and x_2 under abrupt fault, **b** comparison trajectories of y and y_r under abrupt fault, **c** comparison trajectories of e_1 under abrupt fault, **d** comparison trajectories of u under abrupt fault

damping coefficient are represented by the letters D , M , g , and B , respectively. l is the length from the axis of joint to the mass center. τ denotes the torque produced by the motor, u is the voltage applied to the motor or control input. M_m , H_m , and K_m refer to the armature inductance, the armature resistance, and the back electromotive force coefficient, respectively. According to [37], the values of the above physical parameters are given, that is, $D = 1 \text{ Kg m}^2$, $B = 1 \text{ N/(m/s)}$, $Mgl = 1$, $M_m = 0.1H$, $H_m = 1\Omega$, $K_m = 0.2Nm/A$. The purpose of this simulation is to make the moving trajectory of the robotic manipulator track the given reference trajectory in fixed-time under the control of the designed controller and control the tracking error within a small neighborhood near the origin. The given reference trajectory is $y_r = 0.5\sin(t)$.

In view of the system studied in this paper, we introduce the non-affine nonlinear fault into the third-order nonlinear system, so (73) can be rewritten as

$$\begin{cases} \dot{x}_1 = x_2 \\ \dot{x}_2 = x_3 - x_2 - \sin(x_1) \\ \dot{x}_3 = 10u - 2x_2 - 10x_3 + \zeta(t - T_0)\tau(x, u) \\ y = x_1 \end{cases} \quad (74)$$

where $x_1 = q$, $x_2 = \dot{q}$, $x_3 = \ddot{q}$, $\zeta(t - T_0)\tau(x, u)$ is the fault item.

According to (2) and (3), we select the fault time $T_0 = 10s$. At the same time, if the fault type is incipient fault, $q = 8$ is selected, and if the fault type is abrupt fault, $q = +\infty$ is selected. The non-affine nonlinear fault function is uniformly constructed as $\tau = x_1x_2x_3 + \sin(u) + 5$.

For the target system (74), the actual controller and adaptive law are obtained as follows referring to the design process in Sect. 3.1.

$$u = -A_{1,3}e_3^{2p-1} - A_{2,3}e_3^{2q-1} - \frac{1}{2}e_3 - e_2 - \hat{\omega}_3^T \varphi_3 + \dot{\omega} \tag{75}$$

$$\dot{\hat{\theta}}_3 = r_3 e_3 \varphi_3 - R_3 \hat{\omega}_3 \tag{76}$$

In the simulation, the same initial conditions are used, i.e., $x(0) = [0.3, -0.2, 1]$. For the controlled system with incipient fault, the relevant design parameters are selected as $A_{1,1} = 0.5, A_{2,1} = 1, A_{1,2} = 0.5, A_{2,2} = 1, A_{1,3} = 1, A_{2,3} = 20, p = 0.99, q = 1.01, r_2 = 2, r_3 = 2, R_2 = 1, R_3 = 0.8$. Similarly, for the controlled system with abrupt

fault, the relevant design parameters are selected as $A_{1,1} = 0.05, A_{2,1} = 1, A_{1,2} = 1, A_{2,2} = 1, A_{1,3} = 1, A_{2,3} = 20, p = 0.85, q = 1.3, r_2 = 2, r_3 = 2, R_2 = 1, R_3 = 0.6$. The simulation results are shown in Fig. 4. Specifically, Fig. 4a shows the trajectory of the angle, angular velocity, and angular acceleration of the robotic manipulator system with time. Figure 4b shows the tracking error of the robotic manipulator system with the incipient fault and the abrupt fault. Figure 4c is the tracking of the actual output of the system to the given reference output under the schemes proposed, corresponding to Fig. 4b. Figure 4d shows the controller response waveform when the system is subjected to the abrupt fault and the incipient fault under the scheme proposed in this paper.

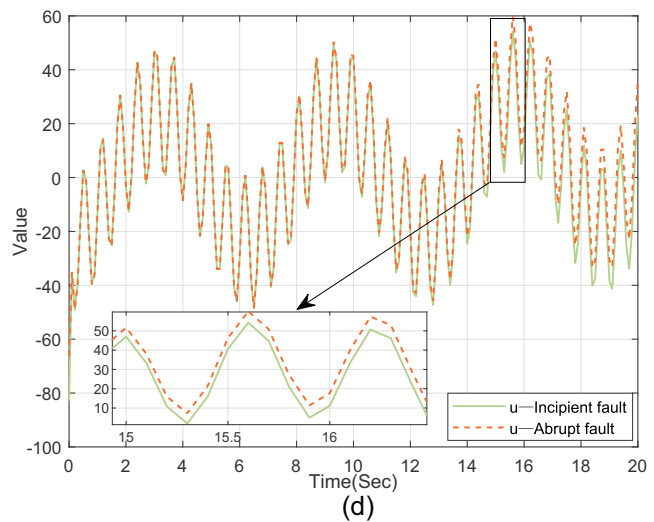
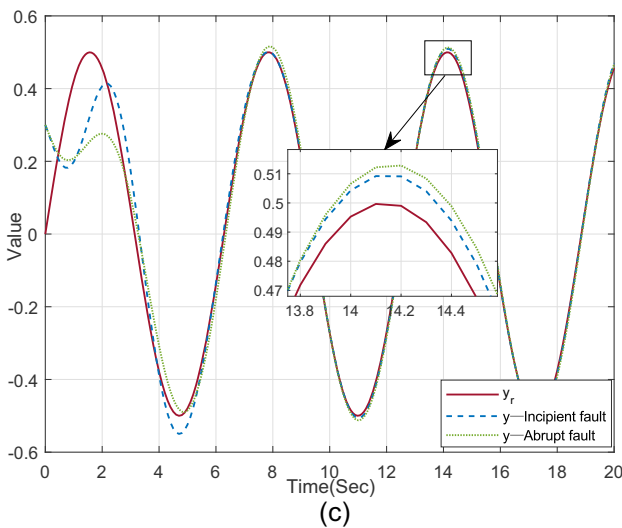
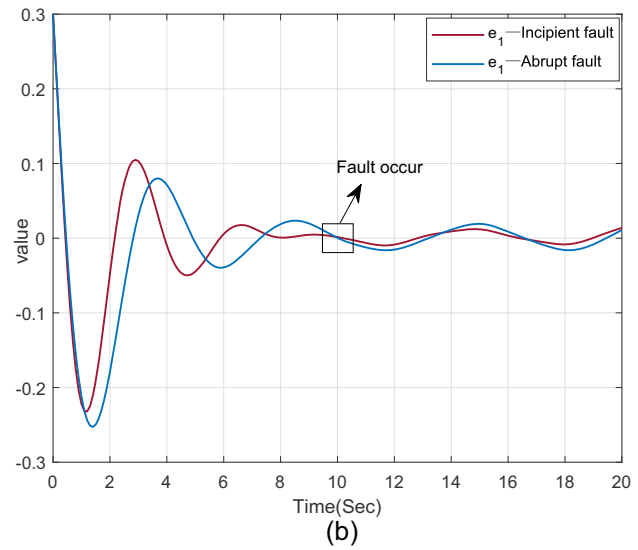
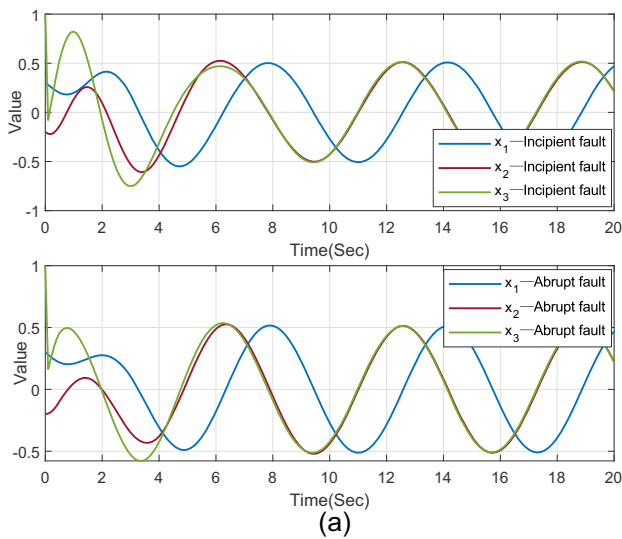


Fig. 4 a Trajectories of $x_1, x_2,$ and x_3 , b Trajectories of e_1 , c Trajectories of y and y_r , d Trajectories of u

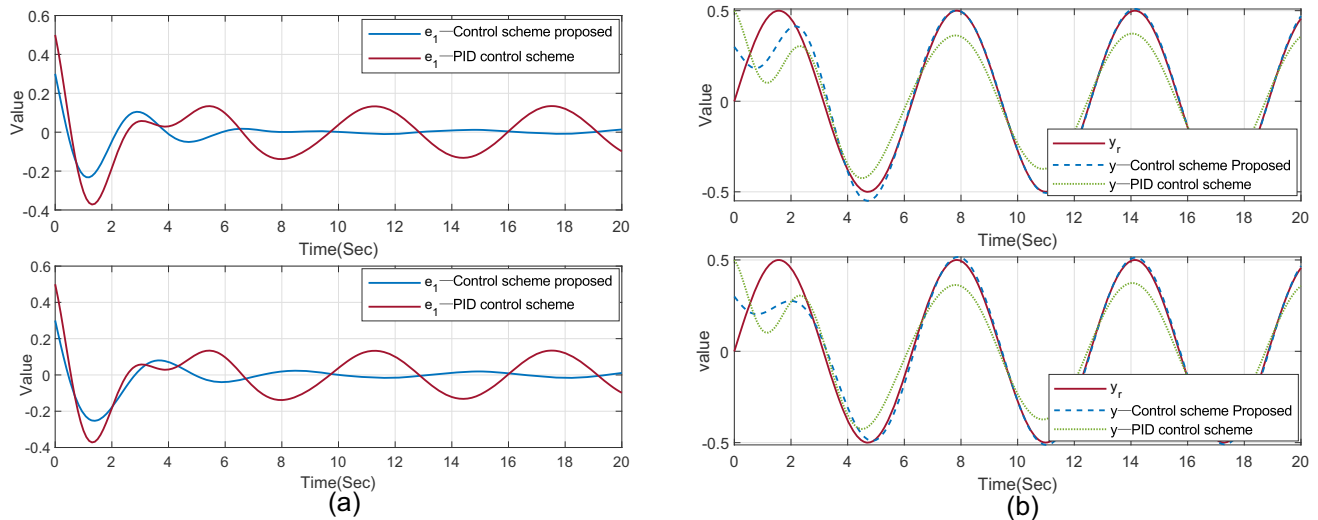


Fig. 5 a Trajectories of e_1 , b Trajectories of y and y_r

In order to further verify the effectiveness of the proposed scheme, the fixed-time fault-tolerant controller based on adaptive fuzzy constructed in this paper is compared with the fuzzy-free PID controller, where PID controller parameters for the robotic manipulator system with the incipient fault are selected as $K_p = 2$, $K_i = 0.23$, $K_d = 0.6$ and PID controller parameters for the robotic manipulator system with the abrupt fault are selected as $K_p = 2.6$, $K_i = 0.47$, $K_d = 0.55$. The comparison results are shown in Fig. 5. Top: comparison results of the system under incipient fault, and Bottom: comparison results of the system under abrupt fault. Specifically, Fig. 5a shows the tracking error under the proposed scheme and the tracking error under the fuzzy-free PID control scheme. Obviously, the scheme proposed in this paper can well ensure the convergence of tracking error, even if the system starts to suffer the impact of actuator fault in the 10s, the tracking performance is not significantly affected. However, since the fuzzy-free PID controller is too sensitive to the parameters, the tracking accuracy will drift obviously and diverge with the increase of time after being disturbed by the actuator fault. Figure 5b shows the tracking of the actual output of the system to the given reference output under the two schemes.

According to the simulation results of Example 1 and Example 2, we can easily get the following conclusions:

- (1) All the variables involved are bounded;
- (2) The proposed fixed-time fault-tolerant control scheme is less affected by faults, which not only ensures the semi-global practical fixed-time stability of the system but also makes the tracking error converge to a small neighborhood near the origin.

5 Conclusion

This paper solves the fixed-time fault-tolerant control problem for nonstrict feedback nonlinear systems with actuator faults by using dynamic surface control technique, adaptive fuzzy technique, and fixed-time stability theory. The fusion of fixed-time control and fault-tolerant control maintains the stability of the controlled system when the actuator fault occurs. The complexity explosion caused by the traditional backstepping method is also mitigated by the introduction of a first-order filter. Meanwhile, the unknown drift term in the system and the non-dynamic effects and changes caused by faults are offset by the application of adaptive fuzzy technique. Finally, the effectiveness of the proposed controller is verified by two simulations. In view of the pursuit of the optimal system performance index while completing the specified tasks and reducing costs in actual production, exploring the optimal control scheme in the sense of fixed-time will be our next research plan.

Acknowledgements This work was supported by the National Natural Science Foundation of China (Grant Nos. 62301212 and 62371182), the Program for Science and Technology Innovation Talents in the University of Henan Province (Grant No. 23HAS-TIT021), the Scientific and Technological Project of Henan Province (Grant Nos. 222102240009 and 222102240067), the Science and Technology Development Plan of Joint Research Program of Henan (Grant No. 225200810007), the Major Science and Technology Projects of Longmen Laboratory (Grant No. 231100220300), the Aeronautical Science Foundation of China (Grant No. 20220001042002), and the Youth Fund Project of Henan Natural Science Foundation (242300420684).

Declarations

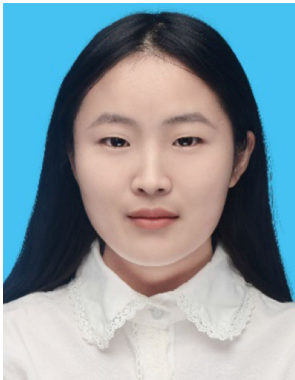
Conflict of interest The authors declare that they have no known competing financial interests or personal relationships that could have appeared to influence the work reported in this paper.

References

- Wang, N., Tao, F.Z., Fu, Z.M., Song, S.Z.: Adaptive fuzzy control for a class of stochastic strict feedback high-order nonlinear systems with full-state constraints. *IEEE Trans. Syst. Man Cybern. Syst.* **52**(1), 205–213 (2022)
- Wang, T., Qiu, J.B., Gao, H.J.: Adaptive neural control of stochastic nonlinear time-delay systems with multiple constraints. *IEEE Trans. Syst. Man Cybern. Syst.* **47**(8), 1875–1883 (2017)
- Zhao, Y.Z., Ma, D., Zhang, Y.W.: Adaptive asymptotic stabilization of uncertain nonstrict feedback nonlinear HOFAs systems with time delays. *Nonlinear Dyn.* **111**(15), 14139–14153 (2023)
- Gao, T.T., Li, T.S., Liu, Y.J., Tong, S.C., Sun, F.C.: Observer-based adaptive fuzzy control of nonstrict feedback nonlinear systems with function constraints. *IEEE Trans. Fuzzy Syst.* **31**(8), 2556–2567 (2023)
- Wang, Y.Y., Tao, F.Z., Fu, Z.M., Wang, N., Chen, Q.H.: Adaptive fuzzy fixed-time dynamic surface control for stochastic nonstrict nonlinear systems with unknown dead-zones. *J. Frankl. Inst.-Eng. Appl. Math.* **360**(6), 4091–4113 (2023)
- Singh, P., Giri, D.K., Ghosh, A.K.: Dynamic surface neuro-backstepping based flight control with asymmetric output constraints. *IEEE Trans. Aerosp. Electron. Syst.* **59**(4), 3859–3870 (2023)
- Wu, J., Chen, X.M., Zhao, Q.J., Li, J., Wu, Z.G.: Adaptive neural dynamic surface control with prespecified tracking accuracy of uncertain stochastic nonstrict-feedback systems. *IEEE T. Cybern.* **52**(5), 3408–3421 (2022)
- Cong, J.P., Hu, J.B., Wang, Y.Y., He, Z.H., Han, L.X.: Fault-tolerant attitude control incorporating reconfiguration control allocation for supersonic tailless aircraft. *Aerospace* **10**(3), 241 (2023)
- Liu, M., Liu, Q.H., Zhang, L.X., Duan, G.R., Cao, X.B.: Adaptive dynamic programming-based fault-tolerant attitude control for flexible spacecraft with limited wireless resources. *Sci. China-Inf. Sci.* **66**(10), 202201 (2023)
- Shi, P.C., Wang, X.Q., Meng, X., He, M.Z., Mao, Y.: Adaptive fault-tolerant control for open-circuit faults in dual three-phase PMSM drives. *IEEE Trans. Power Electron.* **38**(3), 3676–3688 (2023)
- Gassara, H., Boukattaya, M., Hajjaji, A.E.: Polynomial adaptive observer-based fault tolerant control for time delay polynomial fuzzy systems subject to actuator faults. *Int. J. Fuzzy Syst.* **25**(4), 1327–1337 (2023)
- Cui, Y., Duan, G.R., Liu, X.P., Zheng, H.Y.: Adaptive fuzzy fault-tolerant control of high-order nonlinear systems: a fully actuated system approach. *Int. J. Fuzzy Syst.* **25**(5), 1895–1906 (2023)
- Zhang, P., Zhang, J.L., Yang, J.H., Gao, S.: Resilient event-triggered adaptive cooperative fault-tolerant tracking control for multiagent systems under hybrid actuator faults and communication constraints. *IEEE Trans. Aerosp. Electron. Syst.* **59**(3), 3021–3037 (2023)
- Zhang, H.C., Chen, Z.Y., Xiao, B., Li, B.: Fast fixed-time attitude tracking control of spacecraft with prescribed performance. *Int. J. Robust Nonlinear Control.* **33**(10), 5229–5245 (2023)
- Golestani, M., Zhang, W.D., Yang, Y.X., Xuan-Mung, N.: Disturbance observer-based constrained attitude control for flexible spacecraft. *IEEE Trans. Aerosp. Electron. Syst.* **59**(2), 963–972 (2023)
- Zhou, X.Y., Wang, H.P., Wu, K., Zheng, G.: Fixed-time neural network trajectory tracking control for the rigid-flexible coupled robotic mechanisms with large beam-deflections. *Appl. Math. Model.* **118**, 665–691 (2023)
- Sai, H.Y., Xu, Z.B., Xia, C.K., Sun, X.Y.: Approximate continuous fixed-time terminal sliding mode control with prescribed performance for uncertain robotic manipulators. *Nonlinear Dyn.* **110**(1), 431–448 (2022)
- Jia, T.H., Cao, L., Zhang, P.C., Pan, Y.N.: Event-based singularity-free fixed-time fuzzy control for active suspension systems with displacement constraint. *Neural Comput. Appl.* **35**(27), 19751–19763 (2023)
- Jia, T.H., Pan, Y.N., Liang, H.J., Lam, H.K.: Event-based adaptive fixed-time fuzzy control for active vehicle suspension systems with time-varying displacement constraint. *IEEE Trans. Fuzzy Syst.* **30**(8), 2813–2821 (2022)
- Sha, Y.Z., Hu, J., Yao, J.Y.: Active fault-tolerant control strategy for electromechanical servo system based on dual fuzzy RBF neural networks and velocity reconstruction. *Int. J. Fuzzy Syst.* **89**, 47–59 (2022). <https://doi.org/10.1007/s40815-022-01398-6>
- Yang, W., Cui, G., Li, Z., Tao, C.B.: Fuzzy approximation-based adaptive finite-time tracking control for a quadrotor UAV with actuator faults. *Int. J. Fuzzy Syst.* **24**, 3756–3769 (2022)
- Wang, H.Q., Bai, W., Zhao, X.D., Liu, P.X.: Finite-time-prescribed performance-based adaptive fuzzy control for strict-feedback nonlinear systems with dynamic uncertainty and actuator faults. *IEEE T. Cybern.* **52**(7), 6959–6971 (2022)
- Ha, S.M., Liu, H., Li, S.G., Liu, A.J.: Backstepping-based adaptive fuzzy synchronization control for a class of fractional-order chaotic systems with input saturation. *Int. J. Fuzzy Syst.* **21**, 1571–1584 (2019)
- Sheng, N., Zhang, D., Zhang, Q.C.: Fuzzy command filtered backstepping control for nonlinear system with nonlinear faults. *IEEE Access* **9**, 60409–60418 (2021)
- Li, Y.X., Yang, G.H.: Fuzzy adaptive output feedback fault-tolerant tracking control of a class of uncertain nonlinear systems with nonaffine nonlinear faults. *IEEE Trans. Fuzzy Syst.* **24**(1), 223–234 (2016)
- Sun, K.K., Liu, L., Qiu, J.B., Feng, G.: Fuzzy adaptive finite-time fault-tolerant control for strict-feedback nonlinear systems. *IEEE Trans. Fuzzy Syst.* **29**(4), 786–796 (2021)
- Wu, J., Wu, Z.G., Li, J., Wang, G.J., Zhao, H.Y.: Practical adaptive fuzzy control of nonlinear pure-feedback systems with quantized nonlinearity input. *IEEE Trans. Syst. Man Cybern. Syst.* **49**(3), 638–648 (2019)
- Sun, Y.M., Wang, F., Zhang, Y., Chen, C.L.P.: Fixed-time fuzzy control for a class of nonlinear systems. *IEEE Tran. Cybern.* **52**(5), 3880–3887 (2022)
- Zhao, Y., Yao, J.L., Tian, J., Yu, J.B.: Adaptive fixed-time stabilization for a class of nonlinear uncertain systems. *Math. Biosci. Eng.* **20**(5), 8241–8260 (2023)
- Yu, J.J., Yu, H., Li, J., Yan, Y.: Fixed-time stability theorem of stochastic nonlinear systems. *Int. J. Control* **92**(2), 2194–2200 (2019)
- Ba, D.S., Li, Y.X., Tong, S.C.: Fixed-time adaptive neural tracking control for a class of uncertain nonstrict nonlinear systems. *Neurocomputing* **363**, 273–280 (2019)
- Sun, Y.M., Zhang, L.: Fixed-time adaptive fuzzy control for uncertain strict feedback switched systems. *Inf. Sci.* **546**, 742–752 (2021)
- Wang, T., Wu, J., Wang, Y., Ma, M.: Adaptive fuzzy tracking control for a class of strict-feedback nonlinear systems with time-varying input delay and full state constraints. *IEEE Trans. Fuzzy Syst.* **28**(12), 3432–3441 (2020)

34. Farrell, J.A., Polycarpou, M., Sharma, M., Dong, W.J.: Command filtered backstepping. *IEEE Trans. Syst. Man Cybern. Syst.* **54**(6), 1391–1395 (2009)
35. Dong, W., Farrell, J.A., Polycarpou, M.M., Djapic, V., Sharma, M.: Command filtered adaptive backstepping. *IEEE Trans. Control Syst. Technol.* **20**(3), 566–580 (2011)
36. Swaroop, D., Hedrick, J.K., Yip, P.P., Gerdes, J.C.: Dynamic surface control for a class of nonlinear systems. *IEEE Trans. Autom. Control.* **45**(10), 1893–1899 (2000)
37. Wang, H.Q., Liu, K.F., Liu, X.P., Chen, B., Lin, C.: Neural-based adaptive output-feedback control for a class of nonstrict-feedback stochastic nonlinear systems. *IEEE Trans. Cybern.* **45**(9), 1977–1987 (2015)

Springer Nature or its licensor (e.g. a society or other partner) holds exclusive rights to this article under a publishing agreement with the author(s) or other rightsholder(s); author self-archiving of the accepted manuscript version of this article is solely governed by the terms of such publishing agreement and applicable law.



Yueyang Wang received bachelor degree in automation from Jilin Institute of Chemical Technology in 2020 and received M.S. degree from Henan University of Science and Technology in 2023. She is studying for the Ph.D. degree in Control Science and Engineering, Henan University of Science and Technology, Luoyang, China. Her current research interests include nonlinear system, intelligent control, and fixed-time optimization control.



Zhumu Fu has received his B.S. degree from Henan University of Science and Technology in 1998, M.S. degree from Henan University of Science and Technology in 2003, and his Ph.D. degree from Southeast University in 2007. He joined Henan University of Science and Technology in 2007, as a Professor from 2015. His research interests include EMS, PHEV, FCHEV, modeling, analysis and optimization of switched systems, and time-

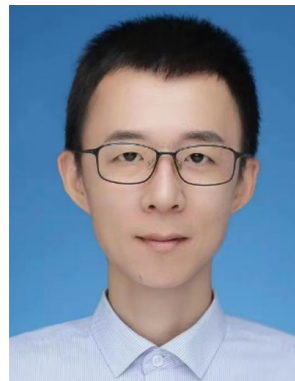
delay systems.



Fazhan Tao has received his B.E. degree from Ludong University in 2010, M.E. degree from Qufu Normal University in 2013, and Ph.D. degree from Engineering Tokyo University of Agriculture and Technology in 2017. He joined Henan University of Science and Technology in 2017. His research interests include robust control for nonlinear systems modeling, analysis and optimization of switched systems and time-delay systems, energy management, and control strategies of electric vehicles.



Nan Wang has received his bachelor degree from Shenyang Institute of Engineering in 2013, M.S. degree from Zhengzhou University in 2018, and Ph.D. degree from Henan University of Science and Technology in 2022. He joined Henan University of Science and Technology as a Lecturer in 2022. His current research interests include nonlinear system and adaptive fuzzy control.



Zhengyu Guo is the Senior Engineer of China Airborne Missile Academy and has the Ph.D. degree. His research interest includes studies on overall design of aircraft and the pre-research of key technologies.